A99-16234

AIAA 99-0333
TEMPORAL PROPERTIES OF MULTIMODE SECONDARY DROPLET BREAKUP

Z. Dai and G.M. Faeth
Department of Aerospace Engineering
The University of Michigan
Ann Arbor, Michigan 48109-2140

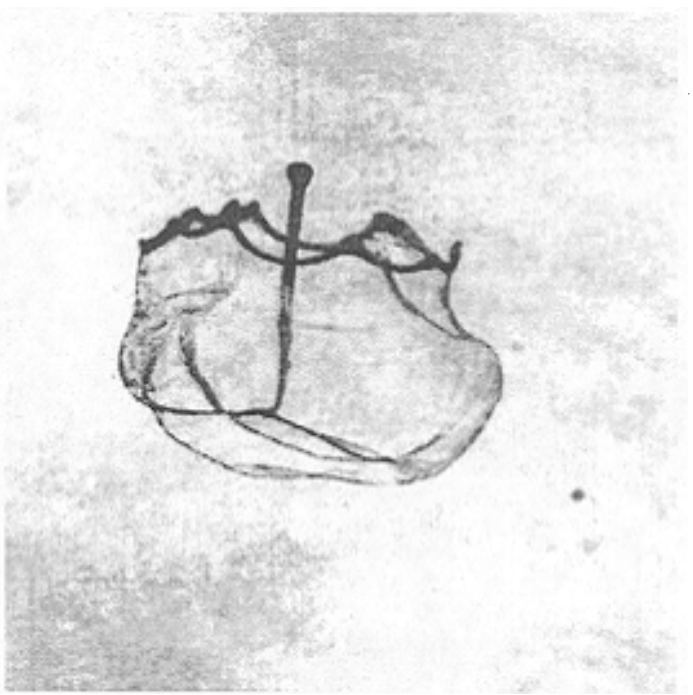

37th AIAA Aerospace Sciences Meeting and Exhibit
January 11-14, 1999 / Reno, NV

TEMPORAL PROPERTIES OF MULTIMODE SECONDARY DROPLET BREAKUP

Z. Dai * and G.M. Faeth †
Department of Aerospace Engineering
The University of Michigan
Ann Arbor, MI 48109-2118, U.S.A.

Abstract

Secondary drop breakup due to shock-wave disturbances was studied for the multimode breakup regime, emphasizing the temperal evolution of breakup. Measurements were carried out in a shock tube using pulsed shadowgraphy and holography to observe the mechanism and outcome of breakup. Test conditions involved liquid/gas density ratios greater than 500, Ohnersorge numbers less than 0.1 and Weber numbers in the range 15-80. The evolution of breakup properties begins with the appearance of a plume droplet at small Weber numbers, the development of plume-like structures due to partial transition into a parent drop and a ligament system at large Weber numbers as the shear breakup regime is approached. Measurements over the test range provided drop sizes, drop velocities and liquid removal rates as a function of time and Weber number in the multimode regime.

Nomenclature

d	=	drop diameter
d_{min}	=	minimum diameter
d_{max}	=	maximum diameter
D_{max}	=	maximum cross-stream diameter
MMD	=	mass median diameter
Oh	=	Ohnesorge number
SMD	=	Sauter mean diameter
t	=	time
t^*	=	characteristic breakup time, $d_o(\rho_L/\rho_G)^{1/2}/u_o$
u	=	streamwise velocity
We	=	Weber number, $\rho_G d_o u_o^2/\sigma$
ρ	=	density
σ	=	surface tension
Subscripts		
e	=	end of breakup
G	=	gas phase property
i	=	onset of breakup
L	=	liquid phase property
o	=	initial state
p	=	parent drop property

Introduction

The secondary breakup of drops is an important fundamental process of sprays. For example, drops formed by primary breakup are intrinsically unstable to secondary breakup, while secondary breakup can be the rate controlling process within dense sprays in much the same way that drop vaporization can be the rate controlling process within dilute sprays[1,2]. Motivated by these observations, Chou et al.[3,4] extended earlier studies of the regimes and outcomes of secondary breakup due to shock-wave disturbances[5,6,7] to consider the evolution of both the properties and rate of formation of drops resulting from secondary breakup as a function of time during breakup in the shear and bag breakup regime. The present study seeks to extend this work to the multimode breakup regime.

Earlier studies of secondary breakup are discussed by Faeth,[1] Wu et al.,[2] Giffen and Muraszew,[8] Hinze,[9] Clift et al.,[10] Krzeczkowski[11] and Wierzba and Takayama,[12,13] among others. Shock wave disturbances were considered during most earlier studies, providing a step change of the ambient environment of the drop, similar to the conditions experienced by drops at the end of primary breakup. The main findings of this work included the conditions required for particular deformation and breakup regimes, the times

* Research Fellow, Member AIAA.
† Professor, Fellow AIAA.

required for the onset and end of breakup, the drag properties of deformed drops, and the drop size and velocity distributions at the end of the breakup process (i.e., the jump conditions). An interesting feature of these results is that secondary breakup extended over appreciable regions of time and space and was not properly described by jump conditions in some instances. This behavior can be illustrated in terms of the characteristic breakup time, t^*, of Ranger and Nicholls[14], defined as follows:

$$t^* = d_o(\rho_L / \rho_G)^{1/2} / u_o \qquad (1)$$

In particular, Liang et al.[15] show that the average breakup time for a wide range of drop conditions is roughly $5.5t^*$, which is comparable to flow residence times within the dense spray region where secondary breakup is dominant process.[1,2] Viewed another way, the original (or parent) drop moves roughly 50 initial drop diameters, while the smallest drops formed by secondary breakup move up to 100 initial drop diameters, during the period of breakup for typical shear breakup processes.[6,7] Such distances can represent a significant fraction of the length of the dense spray region. These observations suggest that the time resolved features of secondary breakup eventually must be understood, i.e., the size and velocity distributions of the drops, and the rate at which liquid is removed from the parent drop, must be known as a function of time during secondary breakup. Motivated by these observations, the present investigation considers the temporal properties (dynamics) of secondary breakup in the multimode breakup regime.

Early studies of the temporal properties of secondary breakup considered the shear breakup regime where secondary breakup proceeds by the stripping of drop liquid from the periphery of the parent drop[3]. Other conditions of the shear breakup study included $\rho_L / \rho_G > 680$, where gas-phase processes approximate quasi-steady behavior, and small Oh number. It was found that the size distributions of drops produced by secondary breakup at each instant of time satisfied the universal root normal distribution function, with MMD/SMD=1.2, due to Simmons.[16] This behavior is very helpful because this two-parameter distribution function is fully defined by the SMD alone, given the MMD/SMD ratio. The properties of drops produced as a function of time included the size and velocities of the parent drop, the SMD and mean and fluctuating velocities of drops produced by secondary breakup, and the rate of liquid removal from the parent drop due to secondary breakup. All these properties were correlated and interpreted using phenomenological theories, providing the information needed to treat shear breakup as a rate process during computations of spray structure.

Subsequent work considered the temporal properties of bag breakup. Various test liquids were used to yield liquid/gas density ratios of 633-893 and Weber numbers of 13-20. It was found that the basal ring formed from the parent drop contains roughly 56% of the initial drop volume and eventually yields drops having mean diameters of roughly 30% of the initial drop diameter while the bag formed contains roughly 44% of the initial drop volume and eventually yields nearly monodisperse drops having mean diameters of roughly 4% of the initial drop diameter. Bag breakup causes significant temporal and spatial dispersion of drops during the breakup period, implying that bag breakup should be treated as a rate process, rather than by jump conditions.

The present study seeks to extend information about the temporal properties of secondary breakup from the shear and bag breakup regime to the multimode breakup regime. Multimode breakup is the most complex secondary breakup regime encountered in typical sprays. The multimode breakup regime is characterized by the appearance of a plume drop near the tip of the bag and the presence of a complex of bag-like and node drop regions. A unifying theme, however, is that the plume drop progressively grows, and the basal ring progressively becomes smaller, as the We increases. Thus, the plume drop eventually evolves into the parent drop of the shear breakup regime while the basal ring correspondingly disappears. Actually, somewhat analogous behavior is observed during the primary breakup of nonturbulent liquid jets in crossflow, see Mazallon et al.[17]

The present measurements were carried out using a shock tube facility, with the environment of test drops during breakup roughly approximating air at standard temperature and pressure (STP). Single and double-pulse shadowgraphy and holography were used to find the properties of the parent

drop, the size and velocity properties of drops produced by secondary breakup and the rate of liquid removal from the parent drop as a function of time during breakup. Test conditions were limited to relatively large liquid/gas density ratios and small Ohnesorge numbers, within the multimode breakup regime where the Weber number range 18-80. As a result, the present test conditions are most representative of multmode breakup within sprays near atmospheric pressure.

The paper begins with a description of experimental methods. Results are then discussed, considering flow visualization, breakup regimes and times, drop deformation, drop sizes, drop velocities and rates of liquid breakup, in turn.

Experimental Methods

Apparatus

The test apparatus will only be described briefly because it was similar to earlier work.[3,4,5,6,7] A shock tube with the driven section open to the atmosphere was used for the measurements, similar to the arrangement used by Ranger and Nicholls.[14] The driven section had a rectangular cross-section (38 mm wide and 64 mm high) and a length of 6.7 m, with the test location 4.0 m from its downstream end. This configuration provided test times of 17-21 ms in the uniform flow region behind the incident shock wave.

The test location had quartz windows (25 mm high and 305 mm long, mounted flush with the interior of the side wall) to allow observation of drop breakup. A vibrating capillary tube drop generator, similar to the arrangement described by Dabora,[18] was used to generate a stream of drops having a constant diameter, and an electrostatic drop selection system, similar to Sangiovanni and Kestin,[19] was used to control of the spacing between drops. This drop stream passed through 6 mm diameter holes in the top and bottom of the driven section of the shock tube at the test location. Test drops had a diameter of 550 μm, while the spacing between drops was at least 20 drop diameters; therefore, drops always were present within the region observed while interactions between adjacent drops during multimode breakup were negligible.

Instrumentation

Single and double-pulse shadowgraphy and holography were used to visualize the secondary breakup process, and to measure the properties of the parent drop and the drops produced by secondary breakup, as a function of time during secondary breakup. The shadowgraphy and holography system were similar to earlier work,[3,4] which involved two frequency doubled YAG lasers (Spectra Physics Model GCR-130, 532 nm wavelength, 7 ns pulse duration, up to 300 mJ per pulse) which could be controlled to provide pulse separations as small as 100 ns. The combined holocamera and reconstuction system allowed objects as small as 3 μm to be observed and as small as 5 μm to be measured with 5% accuracy.

Drop sizes and velocities were measured in the same manner as Hsiang and Faeth.[5,6,7] The diameters of mildly irregular objects were found by measuring their maximum and minimum diameters, d_{max} and d_{min}, through the centroid of the image. Assuming that the drop had an ellipsoidal shape, the drop diameter was taken to be equal to the diameter of a sphere having the same volume as the ellipsoid, e.g., $d^3 = d_{min}^2 d_{max}$. More irregular objects were sized by finding the cross-sectional area and perimeter of the image and proceeding as before for an ellipsoid having the same properties. The velocity of each drop was found by measuring the distance between the centroid of its two images on a double-pulse hologram and dividing by the known time between laser pulses. Results at each condition were summed over at least four realizations, considering 100-200 liquid elements, in order to provide drop diameter and velocity correlations. These sample sizes were smaller than past studies of jump conditions for breakup processes in order to maintain a manageable test program while resolving drop properties as a function of time. Experimental uncertainties caused by the present definition of drop diameters are difficult to quantify, however, they are felt to be small in comparison to the accuracy of the size and distance measurements and sampling limitations. Estimated experimental uncertainties (95% confidence) based on the latter effects are less than 15% for drop diameters and less than 20% for streamwise mean drop velocities.

Test Conditions

The test conditions are summarized in Table 1. Test drops of water were used and the water properties were measured in the same manner as Wu et al.[20] Shock wave Mach numbers in the shock tube were relatively low, less than 1.2; therefore, the physical properties of the gas in the uniform flow region behind the shock wave, where drop breakup occurred, were nearly the same as air at STP.

Results and Discussion

Flow Visualization

Pulsed shadowgraphy flow visualization was used during the first phase of the measurements in order to provide the mechanism and the properties of multimode breakup. Figure 1 is an illustration of a series of these shadowgraphs obtained for water drops having d_o=550μm and We=15,20,33,50,65 and 80. Oh is 0.0045, which places these conditions toward the lower Oh values considered during the present study.[5] Typical results are shown at various values of t/t^* during breakup. The shock wave and flow velocities behind the shock wave are directed from the top to the bottom of the shadowgraphs.

Figure 1a shows typical pictures of bag breakup for a water drop having We=15. Similar to the observations of Chou and Faeth,[4] various conditions during the bag breakup process can be defined as follows: the deformation period where the drop deforms from a spherical to a disk-like shape for t/t^*=0-2; the bag growth period where the center of the disk deforms into a thin membrane-like bag with a much thicker basal ring surrounding its open (upstream) end for t/t^* of 2-3; the bag breakup period where the bag progressively breaks up from its closed downstream end toward the basal ring for t/t^* of 3-3.5; and the ring breakup period where a series of relatively large node drops form along the ring followed by breakup of the ring into a circular array of relatively large drops to end the breakup process for t/t^* of 3.5-4.5. Note that the bag growth and ring breakup periods include a temporal range that is dominated by these processes.

Figure 1b shows typical pictures of breakup for a water drop having We=20. Similar to We=15, the drop deforms to disk-like shape for t/t^* near 1.5 and then the bag grows with the basal ring surrounding its open end. However, as bag grows, a so-called plume drop also grows from the center of the bag; this plume drop can be seen clearly from the picture at t/t^*=2.7. The plume drop is not connected to the basal ring. The existence of plume drop is a characteristic of multimode drop breakup. Measurements reveal that multimode breakup starts at roughly We=18. At this condition, the bag breaks up from t/t^*=2.7 to 3.5. The plume drop separates from the bag at t/t^*=3.0 due to bag breakup. Also note that at t/t^*=3.5, a big drop detaches from the plume drop, which will be called core drop. The basal ring breakup period is from t/t^*=3.5 to 3.8. Then the plume drop breaks up which ends the breakup process.

Figure 1c shows typical pictures of multmode breakup for a water drop having We=25. Similar to We=20, the drop deforms to a disk-like shape for t/t^*=0.0-1.5. At t/t^*=2.3, the bag, basal ring and plume drop can be seen clearly. However the sizes of the bag and basal ring are much smaller while the size of plume drop increases. The bag begins to break up at t/t^*=2.5 and ends breakup before t/t^*=3.0, which is much sooner than observation at smaller We. The basal ring subsequently breaks up and leaves with plume drop at t/t^*=3.5. The plume then undergoes Rayleigh breakup which is finished at t/t^*=5.7. Note that the core drop forms at t/t^*=5.0 and its size increases, but its shape is variable but more or less spherical.

Figure 1d shows pictures of multimode breakup at We=33. The bag finishes breakup sooner than at smaller We, before t/t^* =2.3. The ring and bag size continues to become smaller and the liquid volume inside the plume drop increases dramatically. The core drop forms after the plume finishes breakup, which is different from We=20 and 25 where the core drop forms before the plume finishes breakup. The core drop is no longer spherical. Contrary to the expectation of deforming into a spherical drop without any further breakup, the core drop undergoes Rayleigh breakup and finishes breakup at t/t^*=7.3; therefore the total breakup

time is increased by roughly 60% compared to the breakup times in bag and shear breakup regimes.

Figure 1e shows typical pictures of multmode breakup for a water drop having We=50. The bag and ring still exist, however the volumes of the bag and ring are very small and they finish breakup very quickly. The plume drop breakup is different from We=33 in that the core drop doesn't detach from the main plume; instead, the drops are continuously removed from the plume, resembling the stripping mechanism of the shear breakup mode. In this case the plume drop itself can be viewed as core drop.

Figure 1f shows typical pictures of multimode breakup for a water drop having We=60. The breakup up still belongs to the multimode regime since a bag-like structure can be seen at $t/t^* = 2.0$.

Figure 1g shows typical pictures of breakup for a water drop having We=80. Obviously, there is no bag or plume which means this breakup process belongs to the typical shear breakup regime.

Breakup Regime and Time

Breakup regimes and times are plotted together in Fig. 2. The bag breakup regime is observed for We=13 - 18, multimode breakup for We=18 - 80 and shear breakup for We greater 80. The onset of breakup in the bag breakup regime occurs for t/t^* roughly 3.0, then it decreases progressively to t/t^* roughly 2 in the shear breakup regime. The end of breakup time in the bag breakup regime is t/t^* roughly 4.0, then t/t^* at the end of breakup first increases to maximum of around 7.5 at We=40 and then decreases to 5.0 in the shear breakup regime. Hassler[21] observed similar behavior within the same We range. It is not surprising that the breakup time in the bag and shear regimes is more or less constant, because breakup in the bag regime only involves a bag and ring; in addition, the liquid volume in the bag and ring is fixed, while the shear breakup regime only involves the stripping mechanism. In the multimode breakup regime, however, breakup involves the bag, the ring and the plume, and the liquid volume among three change with We. Therefore, it is understandable that the breakup time cannot be constant. The time for bag and ring breakup is relatively short, roughly one t^*. The increase in breakup time is due to plume breakup. The diameter and liquid volume of the plume increases with increasing We so that its Rayleigh breakup time increases. The contribution of the breakup time for We<40 is also due to the time needed for the breakup of the core drop. For We>40, however, the core drop merges with the plume and the stripping mechanism is more important which causes the breakup time to decrease.

Maximum Cross-Stream Diameter

The maximum cross-stream diameter, normalized by the original drop diameter, is plotted as a function of We in Fig. 3. As We increases, D_{max}/d_o increases slightly, to yield an average value of 2.15 in the multimode regime.

Volume of the Bag, Ring, Plume and Core Drops

The volume of the bag, ring, plume and core drops is plotted as a function of We in Fig. 4. The volume of the bag and ring decrease progressively as We increases and reach very small values at We=40, which implies that after We=40, the bag and ring may not be obvious. The liquid volume in the plume reaches maximum at We=33 and them decreases to zero because the whole plume becomes the core drop for We>40. The liquid volume in the core drop increases continuously and at We=40 its volume is roughly 96% of the original drop volume. The overall behavior of the change of the liquid volume distribution among the bag, the ring, the plume and the core crop corresponds to breakup mode change from bag to shear breakup.

Sizes of Ring, Plume and Core Drops

The SMD/d_o of the ring, plume and core drops is plotted as a function of We in Fig 6. The sizes of bag drops were too small to be measured. Figure 5 shows that the size of ring drops decreases as We increases. The plume doesn't exist in the bag breakup regime so that its volume is zero. For We>40, the plume drops are also very small. The sizes of ring and plume drops are comparable; however, the number of ring drops is much larger than the number of plume drops which is typically around 10 in a

single drop breakup. The core drop doesn't exist in bag breakup regime so that its volume is zero. As We increases, the size of the core drop increases progressively and reaches almost the original drop size at We=40. Note here that the size of core drop is determined from its volume which is measured by collecting all the drops formed from the core drop since the shape of core drop becomes irregular for We>33.

Parent Drop Velocities and Drop Velocities

The velocity of the parent drop, u_p, and the drop velocities, are plotted as a function of normalized time in Fig. 6, similar to Chou and Faeth.[4] For reference purpose, the parent drop velocities for bag breakup, measured by Chou and Faeth[4] are also plotted in Fig 6. The parent drop is defined as all the liquid that is going to breakup further as time increases. Before the onset of the breakup, the parent drop velocity is measured as the whole drop velocity. After the onset of the breakup, the parent drop velocity is taken as the velocity of the leading edge of the parent drop. The parent drop exhibits considerable acceleration during the breakup period, similar to past observations of the motion of parent drops for shear and bag breakup,[4,5,6,7] due to growth of the cross-stream dimensions of the deformed parent drop, as a result of deformation and bag formation, as well as due to increased drag coefficients of the deformed parent drop, both of which significantly increase the drag forces on the parent drop compared to the original spherical drop. The acceleration decreases after the bag breaks up due to sudden release of pressure difference. Drop velocities are much larger than the parent drop velocity because the drop sizes are much smaller than parent drop and tend to accommodate to the continuous phase velocity sooner. Similar to observation of bag breakup,[4] the absolute, u_p, and relative, $(u_o - u_p)$, velocities of the parent drop are comparable at the end of the breakup, which implies a reduction of the relative velocity of the parent drop of roughly 50% during the time of breakup, which is quite substantial.

Mass Removal Rates

As has been described previously, the entire multimode breakup process involves several periods of liquid removal from the parent drop: the first period is associated with breakup of the bag, the second period is associated with breakup of the basal ring and the last period associated with the breakup of plume. During the plume breakup period, for We<40, core drop forms and breaks up; for We>40, drops are continuously removed from the core drop or the plume.

Present measurements of the cumulative volume percentage of liquid removal from the parent drop are plotted in Fig. 7 as a function of the normalized time, because both times of the onset and end of breakup are not constant. It is impossible for the data to collapse, considering the fact that the correlations for the mass removal rates of bag and shear breakup are not the same. Nevertheless, the correlation seen in the figure should be useful for the modeling and simulating spray structure.

Conclusions

Conclusions concerning the temporal properties of secondary drop breakup due to shock-wave disturbances in the multimode breakup regime at small Ohnesorge numbers are summarized in the following for the test conditions given in Table 1:

1. The multimode breakup regime starts at We=18 and ends at We=80. The multimode breakup regime can be subdivided into bag-plume and plume-shear regimes, with transition between these regimes at roughly We=40.

2. As the We number increases, t_i/t^* changes slightly with an average value of 2.3 while t_e/t^* varies and approaches 5.0 when shear breakup regime is approached.

3. The core drop size increases progressively as We number increases and merges with the whole plume for We>40.

4. The liquid volumes in the bag and the ring decrease as We number increases and approach zero at We=40.

5. The mass removal rate resembles bag breakup at lower We and resembles shear breakup at higher We.

Acknowledgements

This research was sponsored by the Air Force Office of Scientific Research, grant no. F49620-95-1-0364, under the technical management of J.M. Tishkoff. The authors would like to thank C.W. Kauffman for the loan of the shock tube facility and advice concerning its operation.

Reference:

1. Faeth, G.M., "Structure and Atomization Properties of Dense Turbulent Sprays, " *Proc. 23rd Symp. (Int.) on Combustion*, The Combustion Institute, Pittsburgh, PA, 1990, pp.1345-1352.

2. Wu, P.-K., Hsiang, L.-P. and Faeth, G.M., "Aerodynamic Effects on Primary and Secondary Breakup, " Prog. Stro. Aero., Vol. 169, 1995, pp.247-279.

3. Chou, W.-H., Hsiang, L.-P. and Faeth, G.M., "Temporal Properties of Drop Breakup in the Shear Breakup Regime, " Int. J. Multiphase Flow, Vol. 23, No. 4, 1997, pp.651-669.

4. Chou, W.-H. and Faeth, G.M., "Temporal Properties of Secondary Drop Breakup in the Bag Breakup Regime, " Int. J. Multiphase Flow, Vol. 24, No. 6, 1998, pp.889-912.

5. Hsiang, L.-P. and Faeth, G.M., "Near-limit Drop Formation and Secondary Breakup, " Int. J. Multiphase Flow, Vol. 18, No.5, 1992, pp.635-652.

6. Hsiang, L.-P. and Faeth, G.M., "Drop Properties after Secondary Breakup, " Int. J. Multiphase Flow, Vol. 19, No. 5, 1993, pp.721-735.

7. Hsiang, L.-P. and Faeth, G.M., "Drop Deformation and Breakup due to Shock Wave and Steady Disturbances, " Int. J. Multiphase Flow, Vol. 21, No. 4, 1995, pp.545-560.

8. Giffen, E. and Muraszew, A., "The Atomziation of Liquid Fuels, " Chapman and Hall, London, 1953.

9. Hinze, J.O., "Fundamentals of the Hydrodynamic Mechanism of Splitting in Dispersion Processes, " AIChE J, Vol.1, 1955, pp.289-295.

10. Clift, R., Grace, J.R. and Weber, M.E., *Bubbles, Drops and Particles*, Academic Press, New York, 1978, pp.26 and 339-347.

11. Krzeczkowski, S.A., "Measurement of Liquid Droplet Disintegration Mechanism, " Int. J. Multiphase Flow, Vol.6, 1980, pp.227-239.

12. Wierzba, A. and Takayama, K., "Experimental Investigation on Liquid Droplet Breakup in a Gas Stream, " Report Inst. High Speed Mech. Tohoku Univ., Vol. 53, No. 382, 1987, pp.1-99.

13. Wierzba, A. and Takayama, K., "Experimental Investigation of the Aerodynamic Breakup of Liquid Drops, " AIAA J., Vol. 26, 1988, pp.1329-1335.

14. Ranger, A.A. and Nicolls, J.A. "The Aerodynamic Shattering of Liquid Drops, " AIAA J. ,Vol. 7, 1969, pp. 285-290.

15. Liang, P.Y., Eastes, T.W. and Gharakhari, A., "Computer Simulations of Drop Deformation and Drop Breakup, " AIAA Paper No. 88-3142, 1988.

16. Simmons, H.C., "The Correlation of Drop-Size Distributions in Fuel Nozzle Sprays, " J. Engrg. Power , Vol. 99, 1977, pp.309-319

17. Mazallon, J., Dai, Z. and Faeth, G.M., "Primary Breakup of Nonturbulent Round Liquid Jets in Gas Crossflow, " Atomization and Sprays, in press.

18. Dabora, E.K., "Production of Monodisperse Sprays, " Rev. Scient. Instru., Vol. 38, 1967, pp.502-506.

19. Sangiovanni, J. and Kestin, A.S., "A Theoretical and Experimental Investigation of the Ignition of Fuel Droplets, " Combust. Sc. Technol., Vol. 6, 1977, pp.59-70.

20. Wu, P.-K., Ruff, G.A. and Faeth, G.M., "Primary Breakup in Liquid/Gas Mixing Layers for Turbulent Liquids, " Atom. Sprays ,Vol. 1, 1991, pp.421-440.

21 Hassler, G., " Breakup of Large Water Drops under the Influence of Aerodynamic Forces in a Steady Stream of Stream and Stream at Subsonic Velocities," *The 3 rd Int. Conf. On Rain Erosion and Related Phenomena*, Hampshire, England, 1970.

Table 1 Summary of the test conditions for multimode breakup

Parameter	Value
Liquid	Water
d_o (μm)	550
ρ_L (kg/m^3)	997
ρ_L/ρ_G (-)	755
μ_L (kg/m-s)	8.94×10^{-4}
σ (N/m)	0.071
Oh (-)	0.045
Re (-)	1670-1910
We (-)	15-80

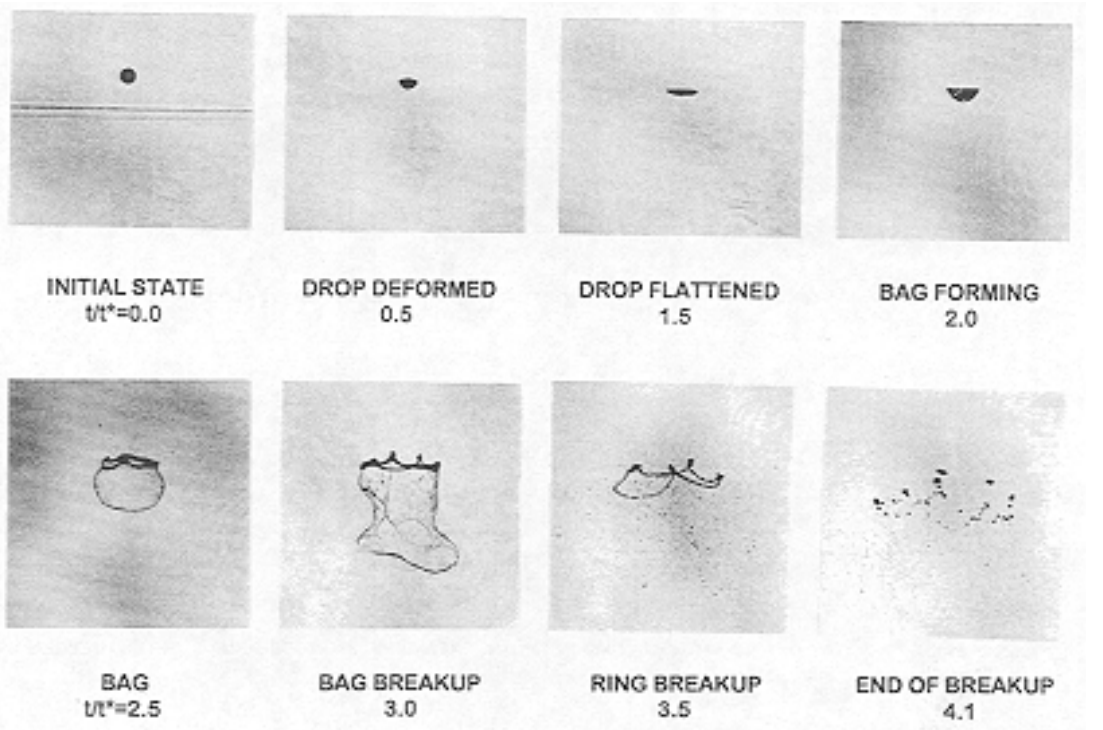

Figure 1a. WATER, We=15, Oh=0.0045

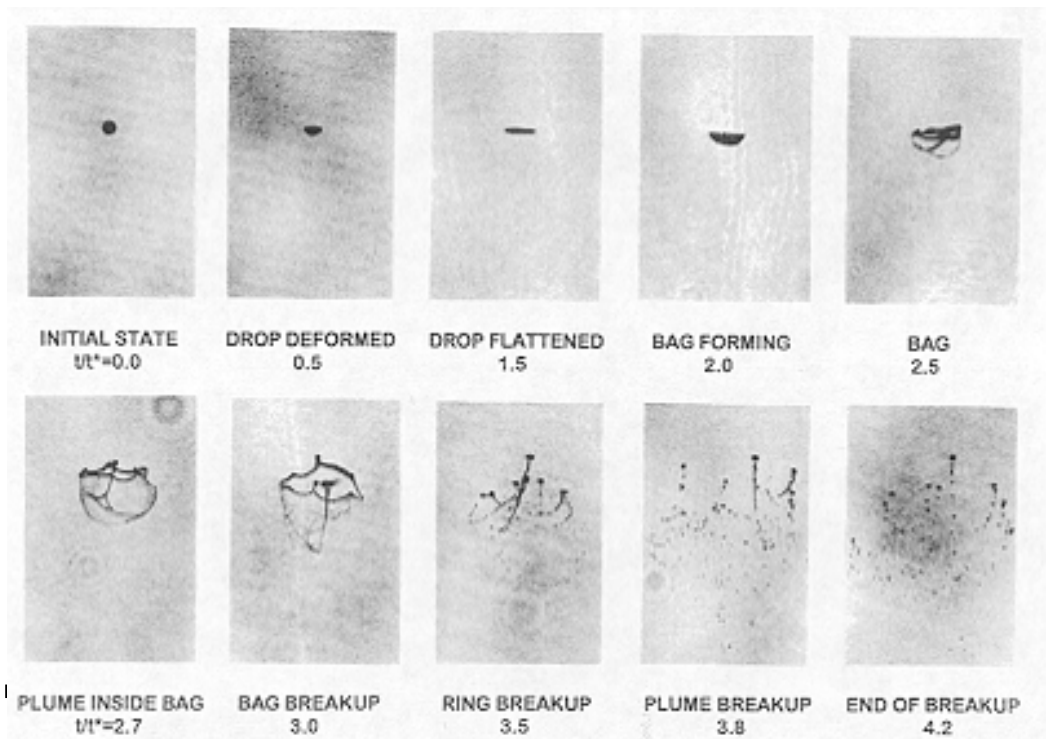

Figure 1b. WATER, We=20, Oh=0.0045

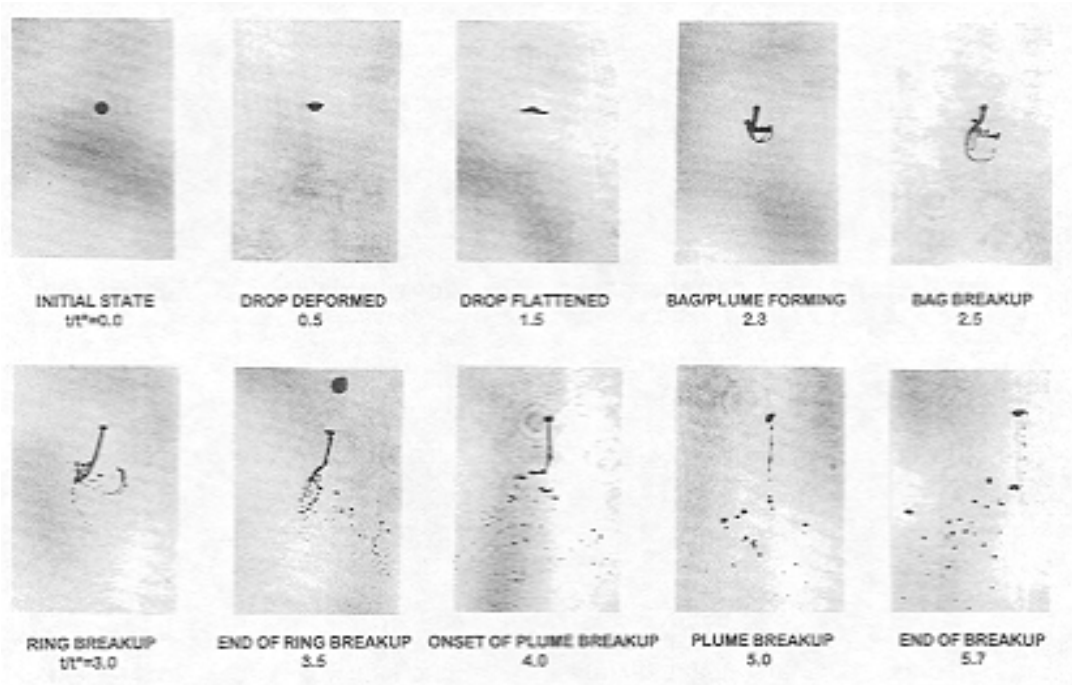

Figure 1c. WATER, We=25, Oh=0.0045

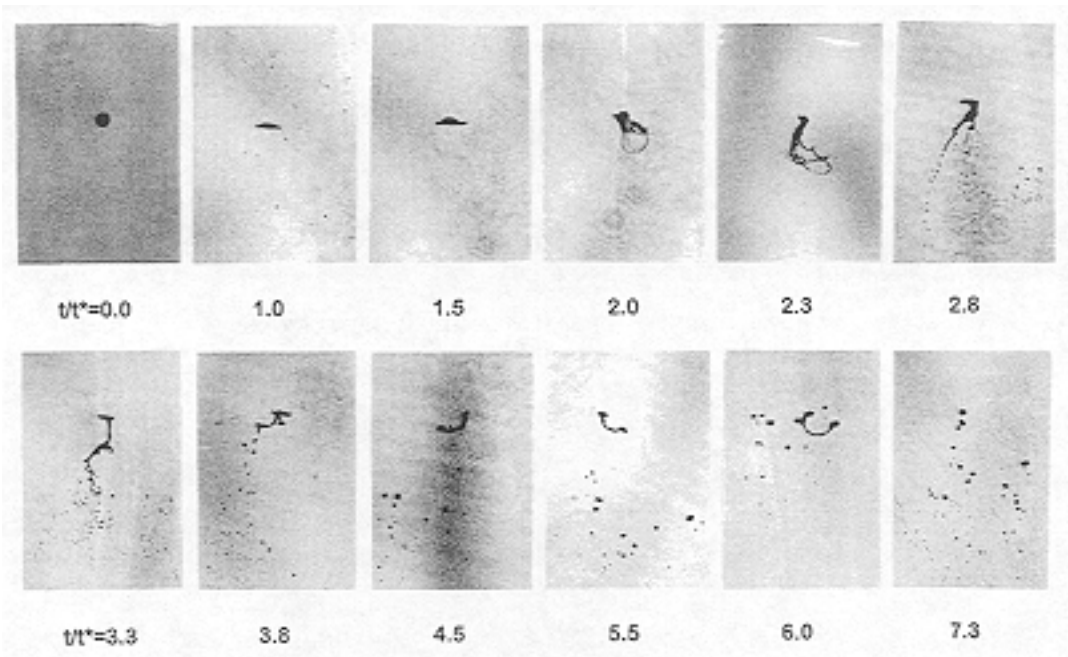

Figure 1d. WATER, We=33, Oh=0.0045

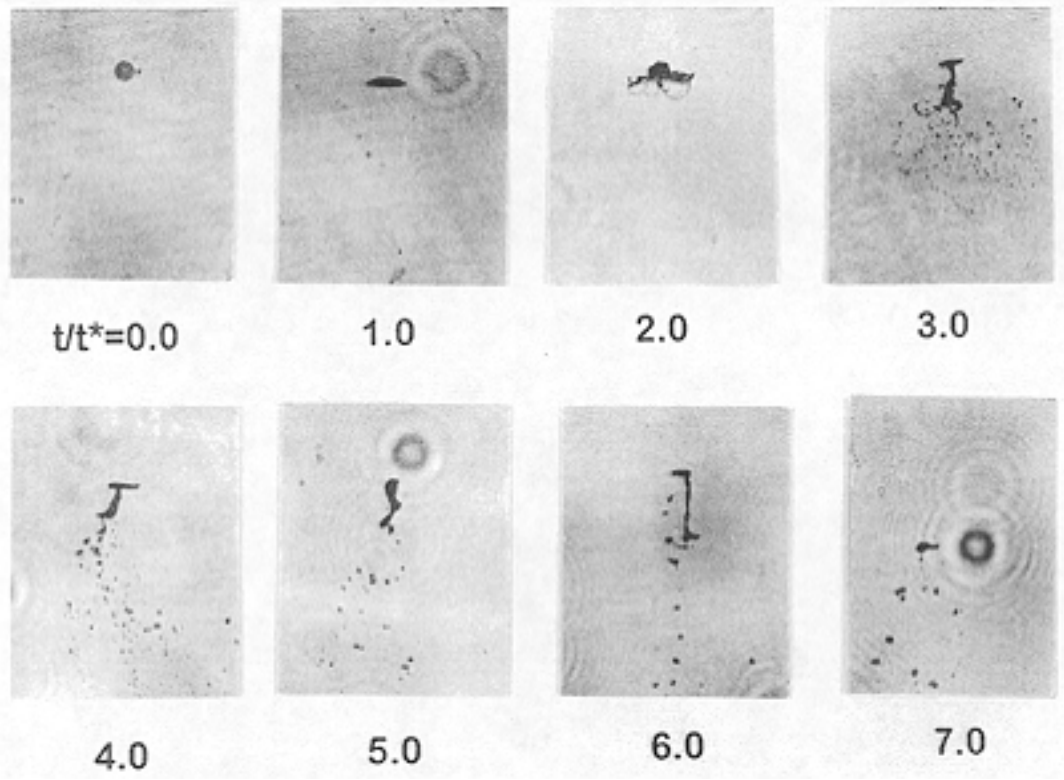

Figure 1e. WATER, We=50, Oh=0.0045

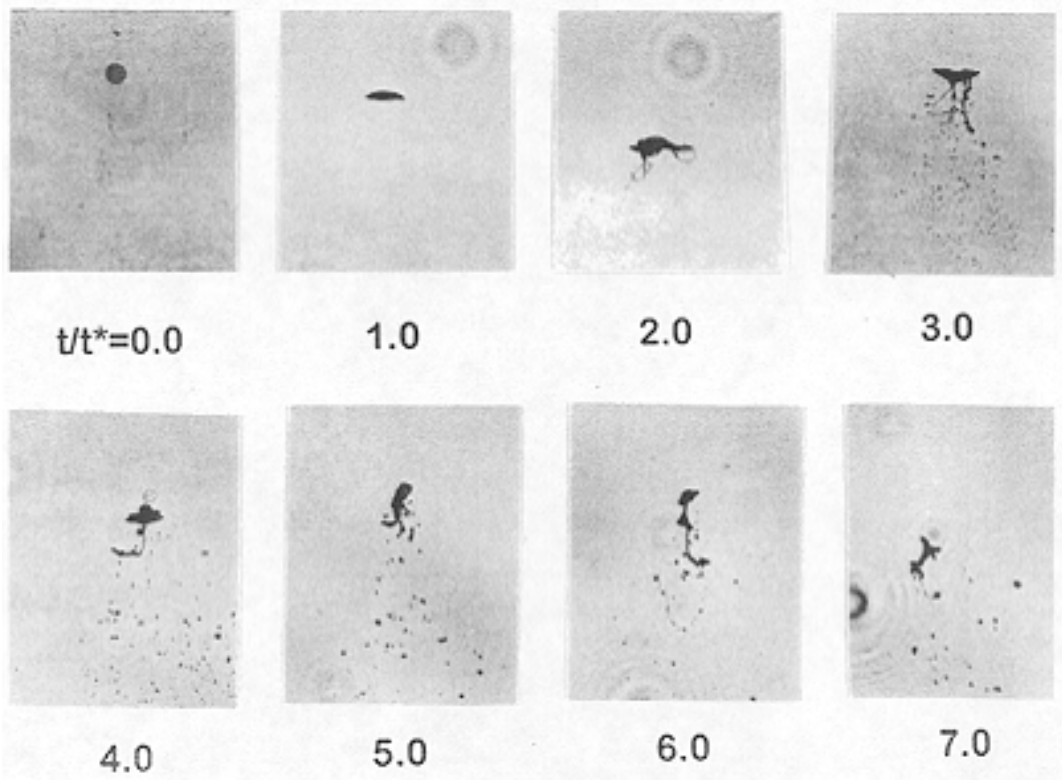

Figure 1f. WATER, We=60, Oh=0.0045

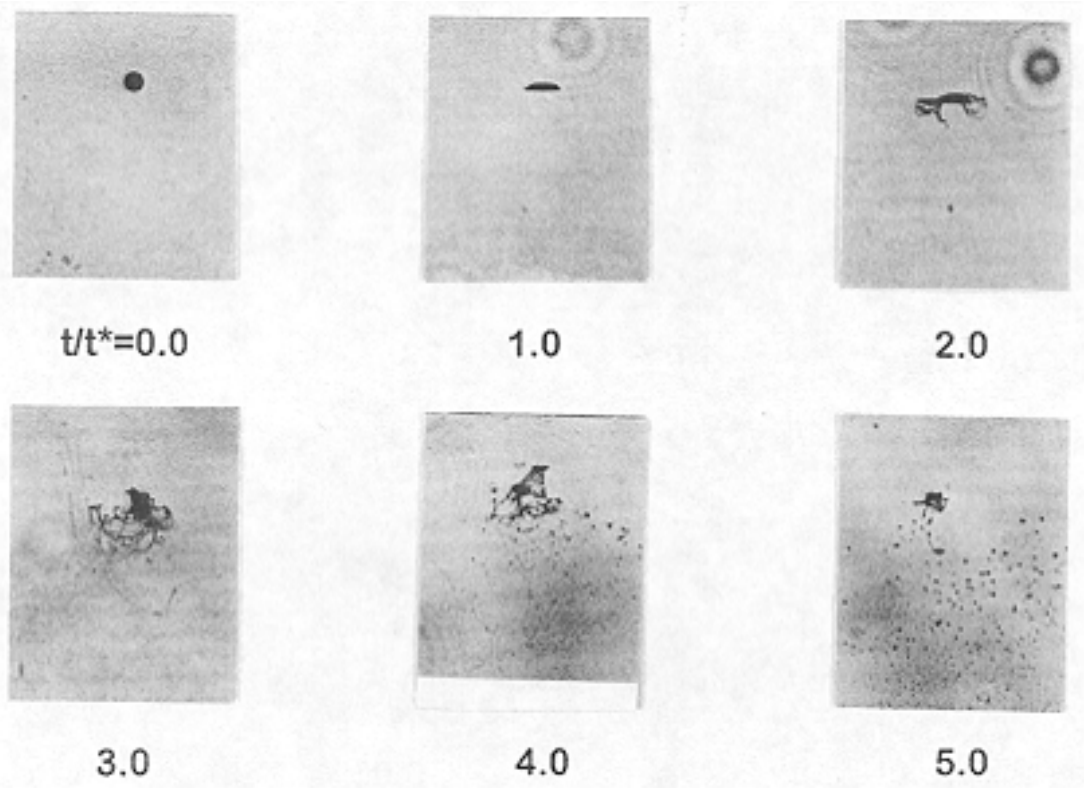

Figure 1g. WATER, We=80, Oh=0.0045

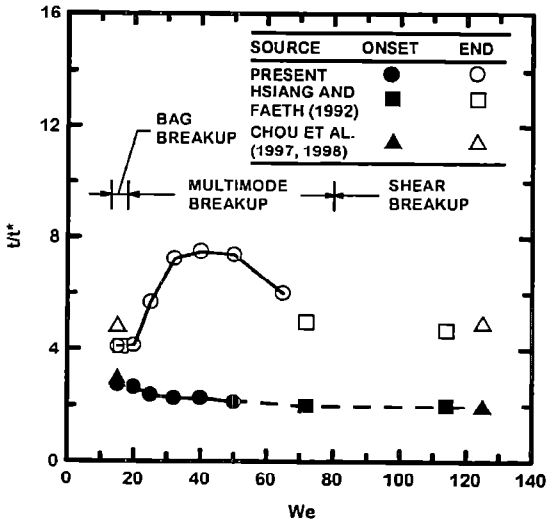

Figure 2 Breakup regimes and times.

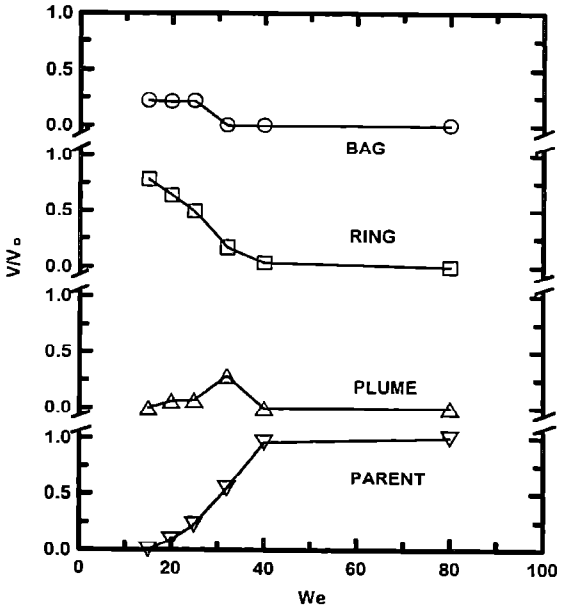

Figure 4 Volume of the Bag, Ring, Plume and Core Drops as a function of We.

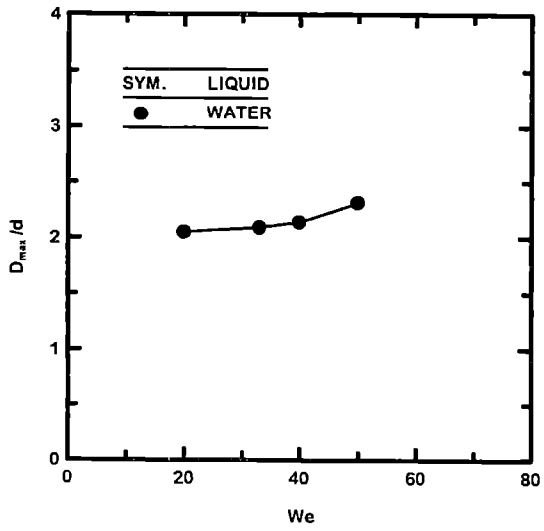

Figure 3 Maximum Cross-Stream Diameter.

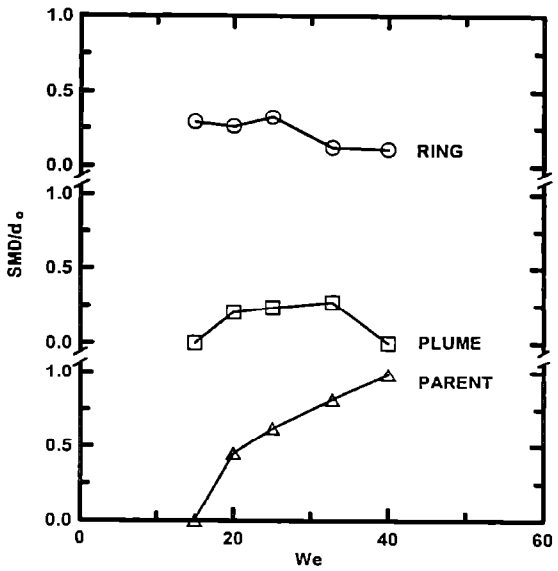

Figure 5 Sizes of Ring, Plume and Core Drops.

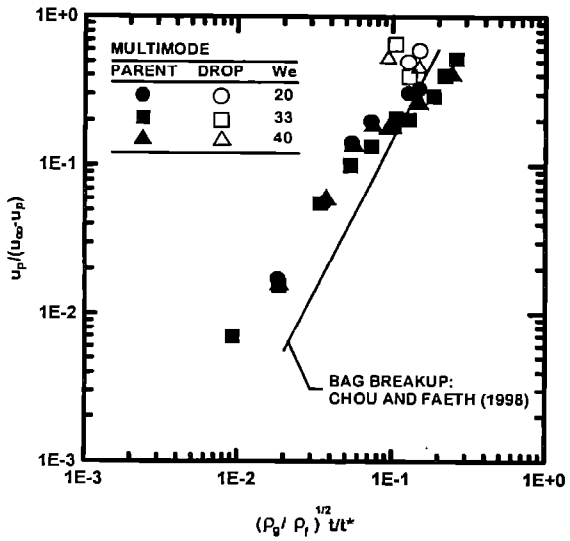

Figure 6 Parent Drop and Drop Velocities.

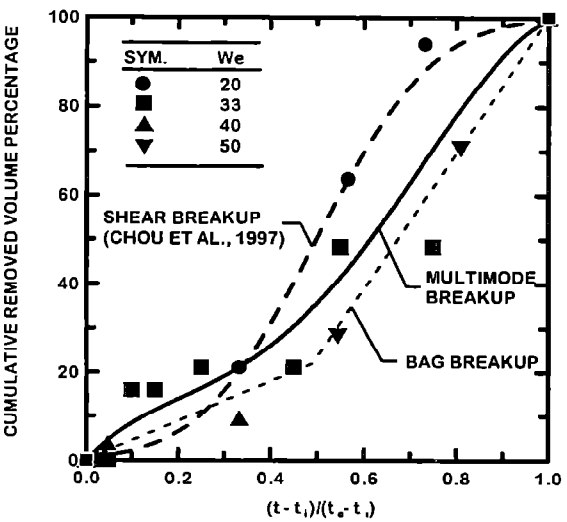

Figure 7 Mass Removal Rates.